©2004 Society of Economic Geologists
Special Publication 11, 2004, pp. 341–357

Chapter 19

Oxidized Gold Skarns in the Nambija District, Ecuador

LLUÍS FONTBOTÉ,† JEAN VALLANCE, AGNÈS MARKOWSKI,*

Section des Sciences de la Terre, University of Geneva, Rue des Maraîchers 13, 1205 Geneva, Switzerland

AND MASSIMO CHIARADIA

School of Earth Sciences, University of Leeds, Leeds LS2 9JT, United Kingdom

Abstract

The Nambija gold district, southeastern Ecuador, consists of oxidized skarns developed mainly in volcaniclastic rocks of the Triassic Piuntza unit, which occurs as a 20-km-long, north-trending, contact-metamorphosed lens within the Jurassic Zamora batholith. High gold grades (10–30 g/t) are accompanied in most mines by very low Fe, Cu, Zn, and Pb sulfide contents. The skarn is constituted dominantly by massive brown garnet (mean Ad_{38}). Subordinate pyroxene-epidote skarn developed mainly at the margins of brown garnet skarn bodies. Mostly idiomorphic and more andraditic garnet (mean Ad_{45}) occurs in blue-green skarn formed as a later phase, in places with high porosity, at the transition with vugs and discontinuous dilational type I veins. The last garnet generations are mainly andraditic and occur largely as honey-yellow to red-brown clusters and cross-cutting bands (mean Ad_{84}). As typical for other skarns developed in volcaniclastic rocks, mineral zoning is poorly defined.

The retrograde overprint is weakly developed, commonly fails to alter the prograde minerals, and is mainly recognized in mineral infilling of structurally controlled (N10°–60°E) vugs and up to several-centimeter-wide type I veins, as well as interstices in blue-green skarn. Retrograde minerals are milky quartz, K-feldspar, calcite, chlorite, and hematite, ±plagioclase, ±muscovite, plus minor amounts of pyrite, chalcopyrite, hematite, sphalerite, and gold. Vugs and type I veins are cut by thin (1–2-mm) throughgoing type II veins that show similar orientations and mineralogy. Native gold is associated with retrograde alteration, mainly in the irregular vugs and type I veins, and subordinately in interstitial spaces and throughgoing type II veins. It is not observed in sulfide-rich type III veins, which cut the previous vein generations.

High-temperature (up to 500°C) and high-salinity (up to 60 wt % NaCl equiv) inclusions in pyroxene represent the best approximation of the fluid responsible for a significant part of the prograde skarn stage. Such a highly saline fluid is interpreted as the result of boiling of a moderately saline (~8–10 wt % NaCl equiv) magmatic fluid at temperatures of ~500°C. Moderate- to low-salinity fluid inclusions (20–2 wt % NaCl equiv) in paragenetically later garnet as well as in epidote and quartz from vugs and type I veins may represent later, slightly lower temperature (420°–350°C) trapping of similar moderately saline fluids with or without some degree of boiling and mixing. The similarity of salinities and homogenization temperatures in late garnet, epidote, and quartz fluid inclusions is consistent with the apparent continuum between the prograde and retrograde skarn stages, as illustrated by the general lack of prograde mineral alteration, even at the contacts with retrograde fillings.

Gold deposition, together with that of small amounts of hematite, chalcopyrite, and pyrite, took place during fluid cooling in the retrograde skarn stages but not during the last retrograde alteration, as indicated by the absence of gold in the sulfide-rich type III veins. The abundance of gold-bearing samples with high hematite/sulfide ratios and generally low total sulfide contents suggests high oxygen fugacities during gold deposition. The northeast structural control of vugs and type I veins, compatible with regional northeast-striking structures, in part with a dilational character, suggests that skarn formation, including gold deposition in the retrograde stage, took place under conditions of tectonic stress.

Minimum Re-Os ages of 145.92 ± 0.46 and 145.58 ± 0.45 Ma for molybdenite from type III veins are compatible with skarn formation and gold mineralization during Late Jurassic magmatism. A genetic relationship with felsic porphyry intrusions that cut the Jurassic Zamora batholith and crop out near several gold skarns is suggested by a published hornblende K-Ar age of 141 ± 5 Ma for a felsic porphyry in the northern part of the Nambija district. Furthermore, the minimum Re-Os ages of ~146 Ma are just slightly younger than the published K-Ar ages (154 ± 5, 157 ± 5 Ma) for the Pangui porphyry copper belt about 70 km north of Nambija.

Resumen

El distrito aurífero de Nambija, suroeste de Ecuador, está constituido por skarns oxidados desarrollados en su mayoría en rocas volcanoclásticas de la unidad triásica de Piuntza, que ocurre como una lente de 20 km de largo afectada por metamorfismo de contacto dentro del batolito de Zamora.

† Corrresponding author: e-mail, lluis.fontbote@terre.unige.ch
*Present address: Institute for Isotope Geology and Mineral Resources, Department of Earth Sciences, 8092 Zürich, Switzerland.

Leyes altas de Au (10-30 g/t) son acompañadas en la mayoría de las minas por contenidos bajos en sulfuros de Fe, Cu, Zn y Pb. El skarn está constituido predominantemente por cuerpos masivos de granate marrón (media Ad_{38}). En menor medida se desarrolla un skarn de piroxeno-epidota en los márgenes de los cuerpos masivos de granate marrón. Granate en general idiomorfo y de composición algo más andradítica (media Ad_{45}) ocurre en un skarn azul-verde formado en una fase más tardía en áreas de alta porosidad situados en la transición entre skarn masivo y cavidades irregulares y vetas dilacionales de tipo I. Las últimas generaciones de granate son predominantemente andradíticas (media Ad_{84}) y forman predominantemente "clusters" y bandas que cortan los otros tipos de skarn. La zonación mineral no está bien desarrollada, lo que es típico de skarns formados sobre rocas volcanoclásticas.

La fase retrógrada es débil, en general no altera los minerales progrados y se reconoce principalmente en los rellenos de cavidades y vetas de tipo I de hasta algunos cm de espesor que están controladas estructuralmente (N10-60°E), así como en intersticios en el skarn azul-verde. Los principales minerales retrógados son cuarzo lechoso, feldespato potásico, calcita, clorita, y hematita, ±plagioclasa, ±muscovita, así como trazas de pirita, calcopirita, hematite, esfalerita y oro. Cavidades y vetillas de tipo I son cortadas por finas (1-2 mm) vetillas de tipo II de similar orientación y mineralogía. El oro nativo está asociado con la alteración retrógrada, principalmente en rellenos de cavidades y venas de tipo I y en menor medida en intersticios y así como en las vetillas cortantes de tipo II. No se observa oro en vetas ricas en sulfuros de tipo III que cortan las generaciones precedentes.

Inclusiones de alta temperatura (hasta 500°C) y alta salinidad (hasta 60% equiv. en peso de NaCl) representan la mejor aproximación al fluido responsable de una parte de la fase prograda. Este fluido muy salino se habría separado por ebullición de un fluido magmático de salinidad moderada (8-10% equiv. en peso de NaCl) a temperaturas de ~500°C. Inclusiones fluidas de salinidad moderada a baja (20-2% equiv. en peso de NaCl) en granate paragenéticamente tardío y en epidota y cuarzo de vetas de tipo I, pueden representar el entrampamiento de fluidos similares de salinidad moderada que pueden haber sido afectados en alguna medida por ebullición y mezcla con otros fluidos. La similitud de salinidades y temperaturas de homogenización de inclusiones fluidas en granate tardío, epidota y cuarzo es compatible con la continuidad aparente entre las fases pro- y retrógrada, que es ilustrada por la poca alteración de los minerales progrados, incluso en contacto con rellenos de minerales retrógrados.

La precipitación de oro, junto a la de pequeñas cantidades de hematita, calcopirita, y pirita, tuvo lugar durante el enfriamiento en la fase retrógrada, pero no en las últimas etapas de ésta, como indica la ausencia de oro en las vetas III ricas en sulfuros. La abundancia de muestras con oro que presentan razones altas de hematita/sulfuros y el contenido en general muy bajo en sulfuros sugieren altas fugacidades de oxígeno durante la precipitación del oro. El control estructural de cavidades y vetas de tipo I, compatible con estructuras regionales de rumbo noreste, y que en parte tienen un carácter dilacional, sugiere que la formación del skarn, incluyendo el depósito de oro en la fase retrógrada, tuvo lugar bajo condiciones de esfuerzo tectónico.

Edades mínimas de Re-Os de 145.92 ± 0.46 y 145.58 ± 0.45 Ma en molibdenitas de vetas de tipo III son compatibles con la formación del skarn y la mineralización de oro durante el magmatismo del Jurásico tardío. Una edad publicada de 141 ± 5 Ma (K-Ar en hornblenda) en un pórfiro félsico en el norte del distrito de Nambija apoyaría una relación genética con las intrusiones porfíricas félsicas que cortan el batolito jurásico de Zamora, y que afloran cerca de varios skarns de oro. Por último, las edades mínimas de Re-Os de 146 Ma son sólo ligéramente más jóvenes que las edades K-Ar publicadas (154 ± 5 Ma. 157 ± Ma) para el cinturón porfírico de Pangui, situado a unos 70 km al norte de Nambija.

Introduction

THE NAMBIJA gold district is located in the Zamora province, southeastern Ecuador, in the Cordillera del Cóndor (Eastern Cordillera) at elevations ranging from 1,600 to 2,300 m (Fig. 1). The district includes, from north to south, the Fortuna, Cambana, Campanillas, Nambija, Guaysimi (also known as Guaysimi Alto), and Sultana del Cóndor mines. These mines comprise several underground and/or open-pit operations, which in part bear other names (Fig. 2).

The gold deposits of the area were exploited by the Spanish conquerors during the 16th century (Prodeminca, 2000), but they were subsequently abandoned and lost in the rainforest. The rediscovery of these bonanza-grade deposits at the end of the 1970s by miners from Portovelo (Fig. 1) led to a gold rush and extensive informal mining. Around 1985, there was a town at Nambija mine with reportedly 20,000 people. During the 1990s, the population decreased as a result of lower gold prices, accidents, and increased pressure to legalize the mining concessions. Today, about 2,000 people extract gold from lodes and placers, either as artisanal miners or belonging to small- and medium-sized companies, mainly at the Nambija mine, and, to a lesser extent, in the other mines of the district. The medium-sized companies include Compañía Minera del Ecuador-Andos at the Nambija mine (El Playón-Mapasingue), Cominza S.A. at the Guaysimi mine, Concumay S.A., at the Campanillas mine, and Compañía Minera Sultana del Cóndor, S.A. at the Sultana del Cóndor mine.

The gold deposits occur mainly in skarn bodies developed in volcano-sedimentary rocks of the Triassic Piuntza unit. Gold grades are typically high (avg 10–30 g/t, up to 1,000 g/t), whereas the contents of Cu, Zn, Pb, and other metals are very low in most mines.

In 1990, total resources of 23 million metric tons (Mt) at 15 g/t (i.e., 355 t Au) were estimated (Mining Magazine, 1990). In 2000, total resources were reevaluated at 125 to 155 t Au and the production since 1980 estimated at 60 to 90 t Au (Prodeminca, 2000).

In a reconnaissance study, Hammarstrom (1992) interpreted the Nambija district as a "gold-associated skarn." Nambija is described by Meinert (1998) as an "oxidized gold skarn" in a worldwide compilation of gold-bearing skarns. The most comprehensive investigation of the geology and ore deposits of the Nambija district was carried out by the British

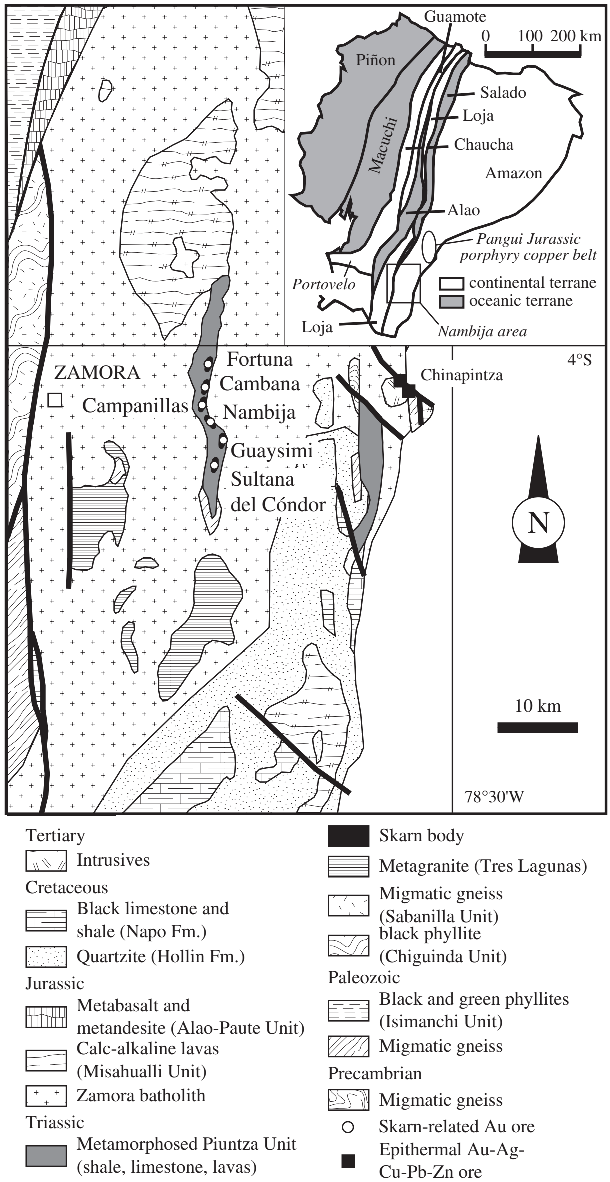

FIG. 1. Regional geologic map of the Nambija region (redrawn from Litherland et al., 1994). The inset is a geotectonic map of Ecuador, showing the Nambija area (redrawn from Litherland et al., 1994).

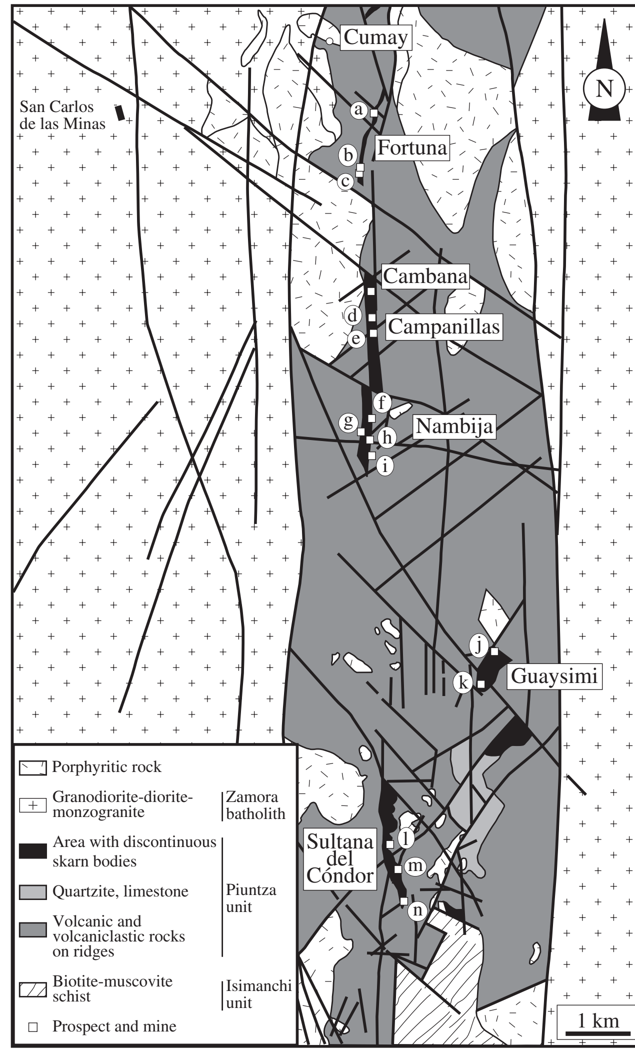

FIG. 2. Simplified geologic map of the Nambija district (modified from Prodeminca, 2000). The Piuntza lithologies occur generally only on topographic highs (ridges), whereas topographic lows (valley bottoms) are commonly underlain by the Zamora batholith, which at this scale cannot be shown. Similarly, the area with discontinuous skarn bodies represents 20 to 30 percent of skarn outcrop at the most. a = Fortuna northern sector, b = Fortuna mine 1, c = Fortuna mine 2, d = Campanillas Katy abandoned workings, e = Campanillas main present workings (open pit and underground), f = Nambija-El Arco (open pit and underground), g = Nambija-El Playón-Mapasingue (underground), h = Nambija-El Tierrero (open pit and underground), i = Nambija-El Diamante (prospect), j = Guaysimi-Banderas (open pit), k = Guaysimi-Central (open pit), l = Sultana del Cóndor-Bruce (open pit and underground), m = Sultana del Cóndor Central (open pit and underground), n = Sultana del Cóndor-Toscón (open pit and underground).

Geological Survey (Litherland et al., 1994; Prodeminca, 2000), who proposed that the gold mineralization overprints skarn bodies "under epithermal conditions." Herein, we present evidence supporting a skarn-related origin for the Nambija gold mineralization.

This paper summarizes the preliminary results of an ongoing study (Markowski, 2003; Vallance et al., 2003). The study does not include comprehensive geologic mapping of the Nambija district, a necessary but not easy undertaking because of the poor outcrop conditions prevailing in a region covered by tropical vegetation. Our study is based on partial mapping of the Fortuna, Guaysimi, and Campanillas mines and selected observations in the Nambija (El Tierrero, Playón, and Mapasingue) and Cambana mines. A total of 278 thin and polished sections were studied, and microprobe (40 samples), XRF (30 samples), and microthermometric analyses (25 samples) were performed. Analytical conditions are detailed in the tables or figures in which the results are presented. More detailed studies on the Fortuna mine and on fluid inclusions from the entire district are in preparation (Markowski et al., in prep; Vallance et al., in prep).

Geologic Setting

Central and western Ecuador consists of a complex mosaic of terranes (Fig. 1), each a few tens of kilometers wide and stretching for several hundreds of kilometers in a north-northeast direction (Aguirre and Atherton, 1987; Feininger, 1987; Mourier et al., 1988a-b; Aguirre, 1992; Aspden and Litherland, 1992; van Thournout et al., 1992; Litherland et al., 1994). These terranes represent geotectonic domains formed during the separation of the North and South American continents in the Triassic.

These domains, of attenuated, oceanic, and continental crust, have been successively reattached to the Amazon craton during subduction of the Pacific plate. Subduction of the Pacific plate or of a proto-Caribbean oceanic plate produced magmatism along the western margin of the Amazon craton during the Jurassic with intrusion of the Zamora batholith and extrusion of the Misahuallí volcanics (Fig. 1). Subsequently, magmatism migrated west due to accretion of microblocks to the continent from southwest to northeast.

The Nambija district is situated at the western margin of the Amazon craton. The skarn bodies are hosted by the Triassic Piuntza unit, which occurs in this area as a north-south–trending contact-metamorphosed lens, ~20 km long and 1 to 2 km wide, within the Jurassic Zamora batholith. The Zamora batholith consists of I-type tonalite and granodiorite (Salazar, 1988; Litherland et al., 1994) and was dated by both Rb-Sr and K-Ar methods at 190 to 140 Ma (Litherland et al., 1994). The main magmatic event is considered to have occurred at 170 to 190 Ma, whereas the younger ages are interpreted as later resetting (Litherland et al., 1994). The Piuntza unit lies unconformably on the Carboniferous Isimanchi unit, which itself lies on the Amazon craton basement and is overlain by the Jurassic Misahuallí unit. The Piuntza unit consists of shallowly dipping continental and/or marine volcano-sedimentary rocks. It is not found farther north in Ecuador, which suggests that it was deposited in a restricted basin (Litherland et al., 1994). In the Nambija district, the Piuntza unit occurs as a flat roof over the Zamora batholith and is mainly preserved as skarn and metamorphosed rocks along the ridges. No detailed stratigraphy is available. According to Paladines and Rosero (1996), the Piuntza unit at the Nambija mine has a minimum thickness of 300 m and includes metamorphosed sandstone, black silty shale, fine- and coarse-grained tuff, volcanic flows, and volcaniclastic breccia as well as limestone and calcareous shale. At sites studied during this work, the Piuntza unit consists mainly of volcaniclastic rocks of basaltic andesite to andesite composition (Markowski, 2003) and quartzite. Two- to 20-cm-thick levels of black silty shale are commonly intercalated with volcaniclastic rocks and quartzite; limestone is only a minor component. The volcaniclastic rocks in places show erosion channels, matrix-supported sedimentary breccia horizons, and synsedimentary tilted blocks. All these features suggest a dominantly continental depositional environment. Litherland et al. (1994) mentioned an increase of the volcanic component to the north of the Nambija district and of marble to the south.

The strike and dip of the Piuntza unit are visible because of the intercalations of black silty shale and grain sorting in volcaniclastic rocks that survived the skarnification. At Fortuna, Cambana, Campanillas, and Guaysimi, bedding strikes dominantly east ±20° with dips of 10° to 50° south. At Nambija, the Piuntza unit forms an east-trending syncline with dips of up to 30°.

Prodeminca (2000, p. 181) identified three main sets of structures in the Nambija district (Fig. 2). The first is constituted by north-south dextral reverse fractures, which limit the district both east and west, and by coeval northeast-striking, steeply dipping fractures with, locally, sinistral displacement. The main gold mineralization is controlled by the northeast-striking fractures, in part as tensional veins. A second set consists of northwest-striking reverse faults and thrust planes dipping 10° to 40° southwest, which cut the previously mineralized structures. Both sets of structures resulted from a northeast-southwest stress field compatible with the oblique northeast-directed subduction that prevailed from the Late Jurassic to Early Tertiary (Litherland et al., 1994). All these structures are crosscut by a third set of east-striking steeply dipping dextral faults.

The Piuntza unit and Zamora batholith are cut by several porphyritic intrusions of felsic composition (Hammarstrom, 1992; Paladines and Rosero, 1996). Immobile element data from Campanillas, Cambana, and Fortuna samples suggest mainly granodioritic compositions and volcanic arc signatures (Markowski, 2003; Markowski et al., in prep.). Several K-Ar determinations give imprecise ages ranging from 145 to 95 Ma (Prodeminca, 2000). An age of 141 ± 5 Ma was obtained on hornblende from a quartz monzonitic porphyry intrusion at the Cu-Mo prospect of Cumay in the northern part of the district (Fig. 2). As discussed later, this age is compatible with results obtained during the present work.

The felsic porphyritic intrusions, including that at Cumay, are frequently altered to quartz-pyrite ± sericite ± K-feldspar ± biotite (Prodeminca, 2000). Pyrite amounts to 3 to 5 percent by volume and as disseminated grains and in network veinlets of 1 to 5 mm thick (e.g., porphyritic intrusion in the Fortuna mine), which extend several tens of meters into the enclosing rocks. Associated with this alteration, Prodeminca (2000) reported porphyry Cu-Mo mineralization at Nambija-El Tierrero and Cumay. Potassic alteration, with shreddy biotite replacing amphibole, was observed in a porphyry dike intruding the Zamora batholith located some 1,000 m west of Cambana along the road to Nambija.

These felsic porphyritic intrusions are recognized within tens to hundred of meters of skarn bodies in several mines, including Fortuna, Cambana, Campanillas-Katy, and Nambija-El Tierrero. However, crosscutting relationships between the porphyritic intrusions and skarn bodies were not observed, except at Campanillas-Katy, where actinolite-epidote endoskarn developed in a poorly exposed porphyritic intrusion. In contrast, at the Cumay Cu-Mo prospect, Prodeminca (2000, p. 120) reported that the dated quartz-monzonite porphyry crosscuts the skarn.

Skarn Types, Vugs, and Veins

In the Nambija district, skarn occurs as massive, coarse-grained, lenticular bodies (Figs. 3–4), which mainly replaced fine-grained volcaniclastic rocks as indicated by field observations and the similar contents of TiO_2, Zr, and other immobile elements in skarn and volcaniclastic rock samples (Markowski et al., in prep.). Carbonate rocks have only been recognized in a few places, including the Nambija-El Diamante prospect (1-m-thick drill hole intersection) and the Guaysimi-Central mine (30-cm-long and 5-cm-thick limestone lens in massive

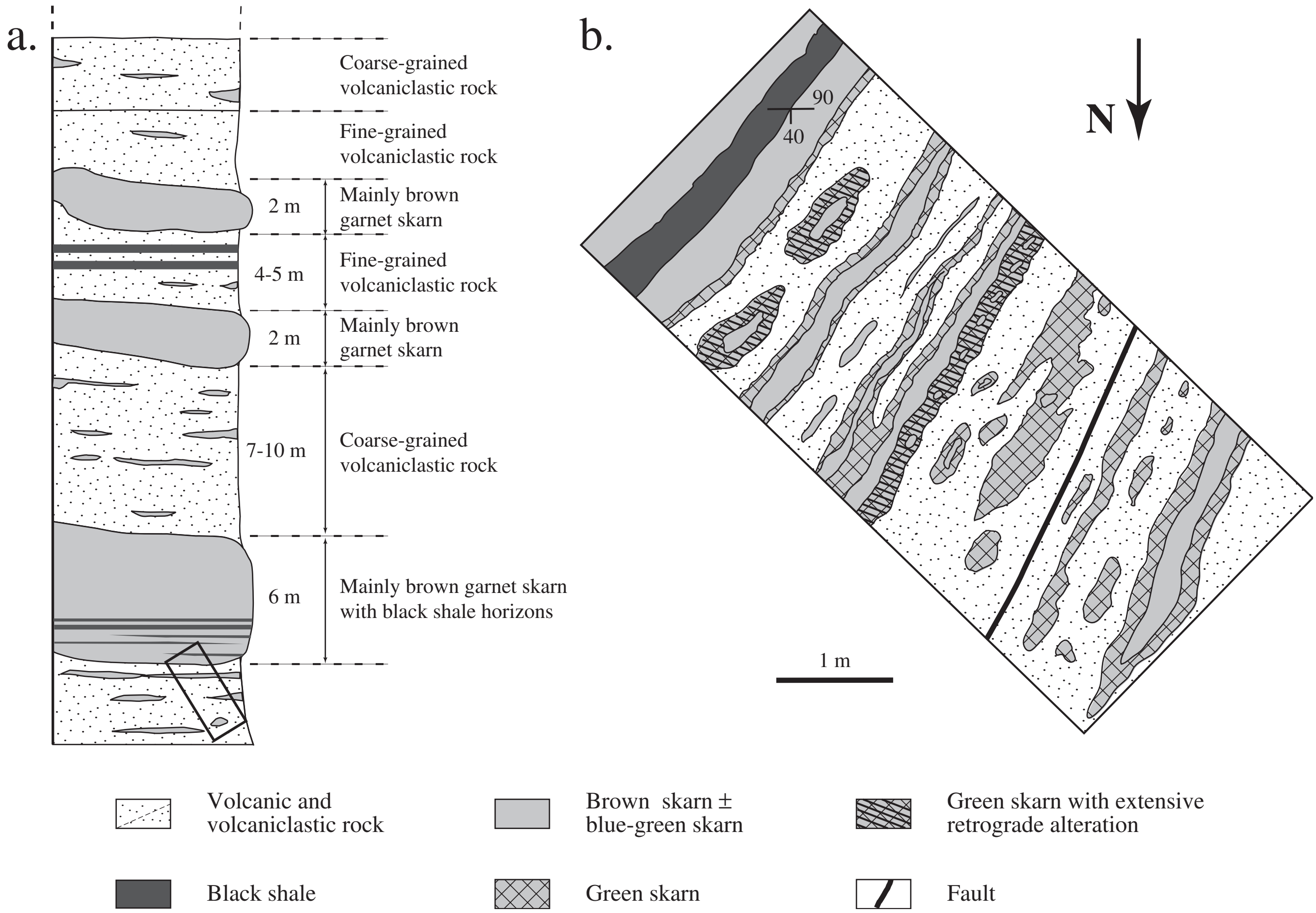

FIG. 3. a. Lithologic column for the Campanillas main open pit, showing the three main skarn bodies. The skarn morphology is controlled by lithology; bedding is revealed by the unskarnified black shale horizons. The black outline shows the location of the map presented in (b). b. Bench map of a typical site including all observed skarn types plus metamorphosed volcaniclastic rocks and black shale intercalations. Green pyroxene-epidote skarn is more affected by retrograde alteration than brown garnet skarn. Bench location is indicated in Figure 8.

garnet skarn). In the latter deposit, bivalve relicts occur in green pyroxene skarn, and at Fortuna bioclasts occur in unskarnified volcaniclastic rocks (Markowski, 2003).

At the outcrop scale, the skarn forms mainly concordant bands a few tens of centimeters to a few meters thick (in Guaysimi-Central up to 10 m; Fig. 4), whose morphology is largely controlled by bedding and unreactive and/or less permeable lithologies like sandstone, black silty shale, and massive volcanic horizons. The transition from skarn to volcaniclastic rocks is usually sharp. The skarn bodies show typical features of metasomatic replacement including irregular limits giving rise to a spotted aspect (Fig. 5a).

The main skarn type is brown garnet skarn consisting of massive coarse-grained garnet ± pyroxene (Figs. 3–5a, b, e). Garnet is anhedral to subhedral (Fig. 5e) and has mainly granditic compositions (mean Ad_{38}, range Ad_{61-20}; Fig. 6; Table 1). It has a dirty appearance, because it replaced volcaniclastic rocks, and contains numerous dark rutile needles. Only locally are garnet cores altered to chlorite, calcite ± hematite during retrograde alteration, with garnet rims remaining unaltered.

A second skarn type, green pyroxene-epidote skarn, consists of pyroxene, epidote ± garnet, and K-feldspar. Pyroxene is mainly diopsidic (Di_{92-47}), with Mn contents that may be significant (Jo_{0-19}). Epidote is locally abundant and, at Fortuna, has Ep_{10-18} compositions (Markowski, 2003). Green pyroxene-epidote skarn occurs generally at the margins of brown garnet skarn bodies as centimetric to decimetric rims (Figs. 3b, 4b). At Guaysimi-Central and mainly Fortuna mine 1 (Markowski et al., in prep), green skarn forms relatively thick bodies mappable at the deposit scale and, at least at Fortuna, are distal relative to the main skarnified area (mine 2). Locally, pyroxene is partly altered to chlorite, calcite ± hematite during retrograde alteration (Fig. 3b).

The proportion of brown skarn bodies displaying a green skarn margin versus direct transition to unskarnified rocks varies from <10 percent at Guaysimi-Central to 50 percent at Campanillas. The contact from green skarn to unskarnified volcaniclastic rocks is commonly marked by a discontinuous, 0.5- to 2-cm-thick rim of K-feldspar, locally also observed at the contacts of brown garnet skarn (Fig. 4b, insets a and d).

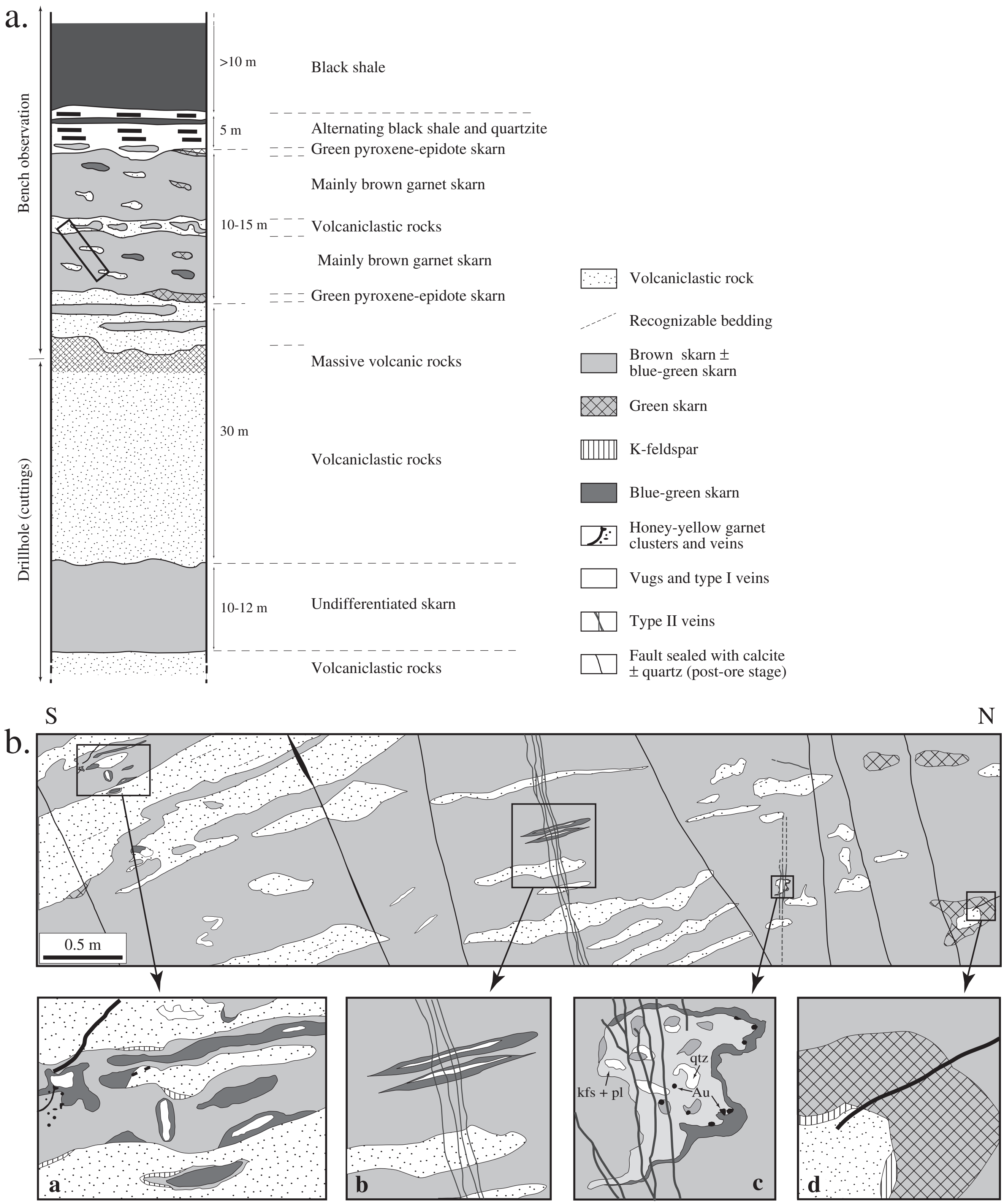

FIG. 4. a. Lithologic column for the Guaysimi-Central mine (9546, 150N, 747,630E). Inset: Location of the detailed bench description shown in (b). b. Bench map, showing relationships between volcaniclastic rocks, skarn types, vugs, and veins. Insets: a. Transition from brown skarn to blue-green skarn and vugs. Volcaniclastic rocks, brown skarn, and blue-green skarn are cut by honey-yellow garnet bands. b. Type I veins crosscut by type II veins. c. Gold-bearing (Au) vug filled with K-feldspar (kfs), plagioclase (pl), and quartz (qtz) and crosscut by type II veins. d. Green skarn between massive brown skarn and volcaniclastic relict; at the contact with the latter there is a discontinuous band of K-feldspar. A honey-yellow garnet band cuts everything.

TABLE 1. Selected Microprobe Analyses (wt %) of Garnet from the Nambija District

Occurrence	Brown garnet skarn		Blue-green garnet skarn		Cluster and veins	
Mean	38.4		45.3		83.7	
Sample no.	DTR 400	DTR 363	DTR 365a	DTR 400	DTR 327	DTR 327
Location	Cambana	Guaysimi-Central			Campanillas	
SiO_2	36.94	38.71	37.65	36.89	37.02	35.17
TiO_2	0.67	0.14	1.59	1.25	0.01	0.03
Al_2O_3	9.52	16.68	13.43	9.60	9.00	0.13
Fe_2O_3	17.79	8.39	11.75	16.84	19.31	31.38
MnO	1.42	1.64	1.71	1.38	1.11	0.79
CaO	33.49	34.20	33.82	33.49	33.29	31.86
Total	99.81	99.77	99.96	99.45	99.72	99.36
Si	2.98	3.00	2.96	2.98	2.99	3.00
Ti	0.04	0.01	0.09	0.08	0.00	0.00
Al	0.90	1.53	1.25	0.91	0.86	0.01
Fe	1.08	0.49	0.70	1.02	1.18	2.01
Mn	0.10	0.11	0.11	0.09	0.08	0.06
Ca	2.89	2.84	2.85	2.90	2.88	2.91
Sum	7.99	7.98	7.97	7.98	7.99	7.99
Cations based on 12 oxygens (mole %)						
Grossular	41.9	72.1	62.0	42.2	39.6	0.0
Andradite	54.2	24.2	34.2	52.9	57.8	98.1
Pyralspite	3.8	3.7	3.8	4.8	2.6	1.9

Notes : Analytical conditions: Current beam 20 nA, acceleration voltage 15 kV

A striking characteristic of the Nambija skarns is the widespread presence of vugs, some elongate, which often grade into 2- to 30-cm-thick discontinuous type I veins aligned in preferential directions (Figs. 5b-d, 7). Vugs and type I veins are filled, in order of decreasing abundance, by anhedral milky quartz, K-feldspar, ±calcite, ±chlorite, ±epidote, ±plagioclase ±muscovite and, in places, by subordinate pyrite, hematite, sphalerite, chalcopyrite, and native gold (Figs. 5h-j), all minerals considered to have precipitated during the retrograde stage (Fig. 8). Vugs and type I veins show gradational contacts with the massive skarn (Fig. 5b), with infill minerals typically cementing euhedral garnet at the vug and/or vein walls (Fig. 5g). This late garnet does not show corrosion against the retrograde minerals. In places, small geodes with clear colorless to purple, subhedral quartz are observed in the center of the veins. In several mines, including Guaysimi, Nambija, Campanillas, and Cambana, the vugs and veins are aligned preferentially along N10° to N60°E directions and have steep dips (Fig. 9a). These orientations are consistent with the northeast-southwest structural control of the gold mineralization reported by Prodeminca (2000) and may represent dilational openings. Alternatively, in places, they are roughly concordant to bedding (Fig. 4b, inset b).

Type I veins also cut volcaniclastic rocks up to a few tens of meters from the skarn front (Fig. 9b), where they have sharper contacts and are narrower than where they cut skarn. The spacing between type I veins ranges from a few to tens of meters (Fig. 9a), and no evidence of vertical movement is observed.

A transition zone of blue-green garnet skarn commonly occurs between brown garnet skarn and vugs and type I veins. It consists of dominantly euhedral garnet, with minor amounts of pyroxene and epidote, cemented by large anhedral grains of quartz and K-feldspar (Figs. 4b, 5b). Garnet is more transparent and shows more andraditic compositions (mean Ad_{45}, range Ad_{99-20}; Fig. 6; Table 1) than that in the massive brown skarn. Some garnet cores are affected by retrograde alteration. Quartz may constitute up to 50 percent and even more of this transition zone. The milky quartz and K-feldspar filling the pores of the blue-green garnet skarn are assigned to the retrograde stage, as also suggested by the transitional position between vugs and/or type I veins and the massive brown garnet skarn. The fact that garnet alteration, typically into chlorite, calcite, ±hematite (Fig. 5f), is more frequent in the blue-green garnet skarn (though still weak and only affecting the cores) supports this interpretation.

The most andraditic compositions are found in honey-yellow to red-brown garnet (mean Ad_{84}, range Ad_{100-46}; Fig. 6; Table 1) that occurs mainly as millimeter-thick, irregular bands (Fig. 5c), which cut all skarn types and volcaniclastic rocks and which, in part, rim vugs and veins typically filled with calcite, chlorite, and quartz (without K-feldspar and gold). Garnet displays strong oscillatory zoning (Fig. 5g), with almost pure andraditic compositions being more abundant toward the rims. Honey-yellow to red-brown garnet also occurs as clusters within the brown garnet skarn giving it a mottled appearance (e.g., right part of Fig. 5b). The clusters are up to 10 mm in diameter but generally smaller.

The different skarn facies and the fillings of vugs and type I veins are frequently crosscut by thin (<1-mm) type II veins displaying sharp contacts (Figs. 5d, 7). They occur mostly as bundles (Figs. 4b, 5d, 9b) and roughly follow the same orientations (N10°–60°E) and dips of type I veins. The infill mineralogy is similar to that of type I veins but with calcite

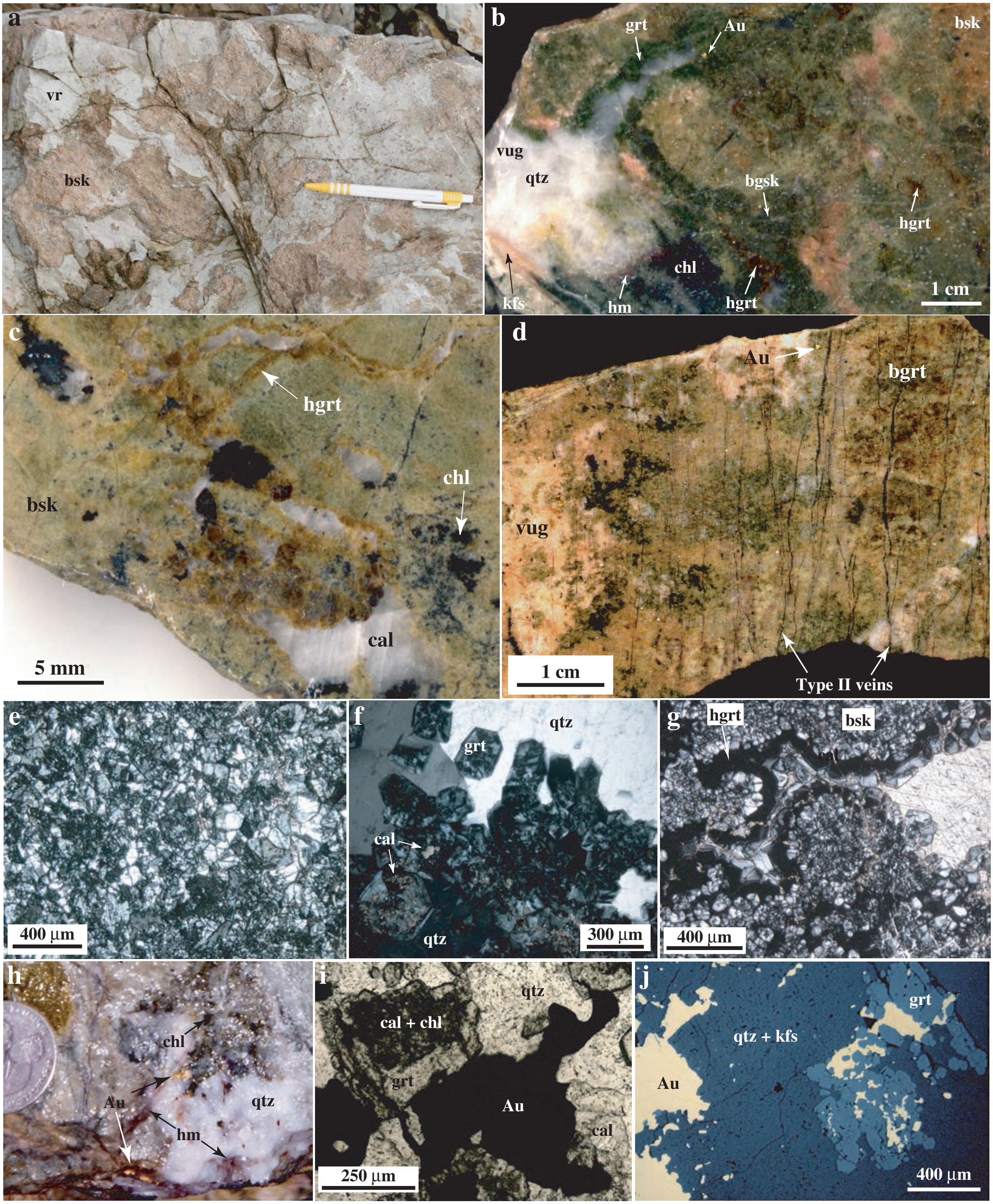
a
vr
bsk
b
grt
Au
bsk
vug
qtz
bgsk
hgrt
chl
kfs
hm
hgrt
1 cm
c
hgrt
chl
bsk
cal
5 mm
d
Au
bgrt
vug
1 cm
Type II veins
e
400 µm
f
qtz
grt
cal
qtz
300 µm
g
hgrt
bsk
400 µm
h
chl
Au
qtz
hm
i
qtz
cal + chl
grt
Au
cal
250 µm
j
grt
qtz + kfs
Au
400 µm

present and sulfides slightly more abundant (but still <5%). A key difference from type I veins is their throughgoing character. Type II veins are observed in all deposits studied except Fortuna. A later vein generation comprises steeply dipping N70°- to 100°E-trending type III veins, which cut vugs and types I and II veins (Fig. 7). They are much richer in sulfides, typically granular pyrite (5–50 vol %), and in places they contain sphalerite and molybdenite. Other infill minerals are similar to those in type II veins. Their thickness ranges from 1 to 2 mm but can reach a few centimeters. At Guaysimi-Central, type III veins cutting volcaniclastic rocks show an alteration halo of chlorite and calcite ±epidote.

At Guaysimi-Banderas (Fig. 2), steep 1- to 2-mm (up to 1-cm)-wide type III veins cut volcaniclastic rocks, are filled by quartz and granular pyrite, and display quartz-sericite halos similar to the D veins defined by Gustafson and Hunt (1975) in the porphyry copper environment. Such quartz-sericite alteration is not recognized in the skarn.

Sealing of N10°- to 70°E-striking late normal faults (vertical movement of centimeters to meters) by calcite ± quartz (Fig. 5b) constitutes the last vein generation. At Guasysimi-Central, these calcite veins are cut by east- to southeast-trending reverse faults dipping at 10° to 40° south.

Mineralization and Ore Geochemistry

Native gold, in grains up to several millimeters in size, together with retrograde quartz, K-feldspar, garnet, and calcite, occurs preferentially in vugs (Fig. 5b) but mainly in type I veins in skarn bodies (Figs. 4b inset c, 5h-j, 9b). Subordinately, gold occurs in type II veins but is not observed in type III veins. Some gold occupies an interstitial position between garnet and pyroxene grains in skarn affected by retrograde alteration but lacking vugs and veins, as frequently observed in blue-green garnet skarn. Retrograde alteration is generally weak and, in places, is expressed only by quartz, K-feldspar, and calcite filling interstitial spaces between unaltered garnet and pyroxene grains (Fig. 5j). Thus, cursory observation could lead to the erroneous conclusion that gold occurs in unaltered skarn.

Type I veins are also gold bearing where crosscutting volcaniclastic rocks but, like the type I veins themselves, always within a few tens of meters distance from the skarn front. At Sultana del Cóndor (Fig. 2), gold is reported to occur in fractures up to a few meters from the skarn bodies, always "associated to K-feldspar alteration" (Prodeminca, 2000, p. 109; A. Eguez, pers. commun., 2003). Gold contains 1 to 15 wt percent Ag and <1 wt percent Hg (Litherland et al., 1994; Paladines and Rosero, 1996; Prodeminca, 2000; Markowski, 2003).

Hematite is a subordinate mineral at Nambija but is relatively common in vugs and type I veins, typically as the only opaque mineral in addition to native gold (Fig. 5h). In contrast, although some pyrite, chalcopyrite, and sphalerite are found together with gold, the presence of native gold does not correlate with total sulfides. The native gold is often observed in vugs and type I veins devoid of sulfide minerals, and the sulfide-rich type III veins are barren.

The total amount of sulfide minerals (pyrite > chalcopyrite > sphalerite) is remarkably low in the Nambija deposits, typically <1 percent, and in numerous mineralized samples visible sulfide minerals are absent. As noted above, the content of sulfide minerals increases progressively from type I to type III veins.

Sphalerite abundance is variable: traces are found in vugs and type I veins at Campanillas and Guaysimi; larger amounts occur as disseminated grains forming centimeter-thick bands along the inner side of the skarn front against limestone at Nambija-El Diamante, where grades of >5 percent Zn are reported (Cooperativa 11 de Julio and Gribipe, 2000). Similar sphalerite disseminations are also observed in volcaniclastic rocks a few centimeters from the skarn front at Campanillas.

Major and trace element analyses were performed on 50 selected mineralized samples (300–1,000 g each) by XRF and neutron activation and on some gold-rich samples by fire assay with gravimetric finish. Bismuth and Te were analyzed by atomic absorption. The results are presented in Figure 10 and Table 2, which includes the analytical details. Because of the limited size of the analyzed samples, the results are only indicative and true metal contents cannot be inferred from them.

The highest gold contents were observed in samples from vugs and type I veins at Guaysimi (up to 1,020 ppm) and Campanillas. The low total sulfide contents are reflected by chemical analyses. All but two samples have <1 and most <0.1 wt percent S. In support of the petrographic observations, gold does not correlate with Cu, Zn, S, and As (Fig. 10). As shown in Figure 10c, gold-rich samples (Au >100 ppb) frequently possess S, Cu, and Zn contents of <100 ppm. Some samples show even higher Au than Cu and Zn contents (e.g., sample DTR 105; Table 2).

FIG. 5. Typical skarn and gold mineralization in the Nambija district. a. Spots of brown skarn (bsk) in volcaniclastic rocks (vr) in the Guaysimi-Central mine. b. Transition from brown skarn to blue-green skarn (bgsk) and vugs. Honey-yellow garnet clusters (hgrt) occur in the brown and blue-green skarn. The vug on the left is filled with late garnet (grt), K-feldspar (kfs), quartz (qtz), hematite (hm), and chlorite (chl). Native gold grains (Au) occur preferentially at the contact between garnet and quartz (Campanillas main present open pit, sample DTR 380). c. Honey-yellow garnet bands in brown garnet skarn. In part they form a rim around vugs filled by calcite and chlorite. (Campanillas main present open pit, sample DTR 327). d. Type II veins crosscutting brown skarn, blue-green skarn, and vugs at Guaysimi-Central mine. Vugs and type II veins contain gold (sample DTR 305). e. Anhedral to subhedral anisotropic garnet in brown garnet skarn (Campanillas main present open pit, sample DTR 380, transmitted light). f. Idiomorphic garnet cemented by milky quartz in blue-green garnet skarn. Garnet cores have calcite (cal) inclusions, product of weak retrograde alteration (Campanillas main present open pit, sample DTR 380, transmitted light). g. Honey-yellow garnet band in brown garnet skarn, showing zoning from grandite (anisotropic bands) to pure andradite (isotropic rim). The vein grades laterally into a vug filled by calcite (Campanillas main present open pit, sample DTR 327). h. Outcrop of gold-bearing type I vein in the Campanillas main present open pit. The vein is filled with quartz, hematite, and chlorite. i. Gold between garnet, quartz, and calcite in type I vein at the Guaysimi-Central mine. The garnet core shows retrograde alteration to calcite and chlorite (sample DTR 305, transmitted light). j. Gold together with late garnet, quartz, and K-feldspar in a type I vein at the Guaysimi-Central mine (sample DTR 305, reflected light).

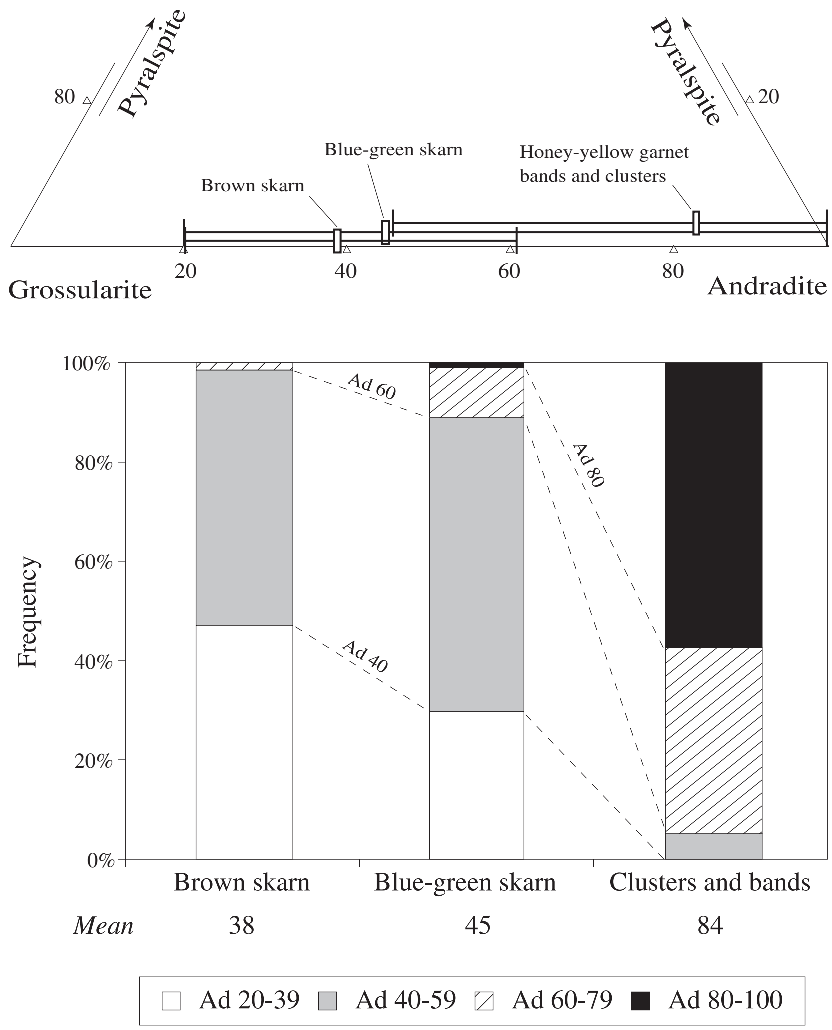

FIG. 6. Composition of garnet (mole %) from different skarn types in the Nambija district. Samples from the Cambana (n = 77), Campanillas (n = 146), Nambija (n = 295), and Guaysimi (n = 155) mines. See Table 1.

Antimony and As contents are also very low (Sb <10 ppm, As <120 ppm; Fig. 10e). Amtimony is more abundant in the green pyroxene-epidote skarn and As in the brown garnet and blue-green garnet skarn. At Fortuna, green pyroxene skarn is interpreted to occupy a distal position with respect to the main skarn area (Markowski et al., in prep). Although Litherland et al. (1994, p. 93) documented the presence of Bi tellurides intergrown with gold at Campanillas, the contents of Bi and Te are also extremely low (<10 ppm) in the analyzed samples.

Fluid Inclusions

The first stages of an ongoing fluid inclusion study investigated prograde garnet and pyroxene, retrograde epidote, and quartz in vugs and type I veins, as well as calcite (sealing normal faults) from Fortuna (n = 63), Cambana (n = 34), Campanillas (n = 44), Nambija (n = 19), and Guaysimi (n = 62). Late blue-green skarn garnet and honey-yellow garnet contain suitable inclusions, but the early and volumetrically dominant brown skarn garnet is too dirty and opaque for meaningful fluid inclusion study. Heating and freezing analyses were obtained on ~100-μm-thick, doubly polished rock sections with a Linkam stage, as described by Shepherd (1981).

The results are similar for all studied deposits. Five fluid inclusion types are distinguished (Fig. 11). Inclusions containing at least one solid phase are termed Lh. Two-phase fluid inclusions (L) show a decrease of the V/L ratio as their homogenization temperatures decrease (L1–L3). Vapor-rich fluid inclusions show V/L ratios between 0.9 and 1. All fluid inclusions show eutectic temperatures below –40°C, indicating the presence of cations like Ca^{2+}, Mg^{2+}, or Fe^{2+}/Fe^{3+}.

The salinity vs. T_h plot (Fig. 11) shows a group of high-temperature inclusions (mainly ~400°–500°C) occurring both in prograde pyroxene and garnet and retrograde quartz and epidote. Another group occurs as secondary L3 and Lh lower temperature inclusions (<300°C) in quartz.

The pyroxene fluid inclusions (Lh) record the highest homogenization temperatures (mainly 500°–430°C) and salinities (12–60 wt % NaCl equiv). Inclusions in garnet (L1-2) are of slightly lower temperature (mainly 480°–390°C) and salinity (20.2–2.6 wt % NaCl equiv), with those in garnet from blue-green skarn displaying higher temperatures and

VUGS AND VEINS IN THE NAMBIJA DISTRICT

		Key features	Observations
Vugs	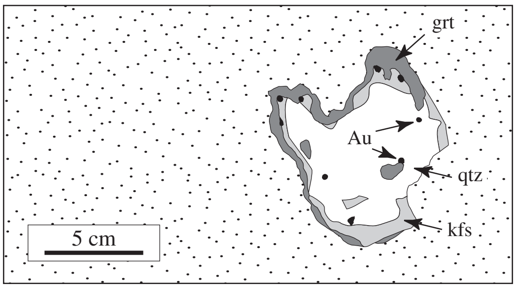	Vugs and type I veins (N10-60°E) show irregular and discontinuous morphology with gradational contacts to massive skarn (the infilling minerals typically cement euhedral garnet at the vug/vein wall) **Filling:** mainly quartz, K-feldspar, calcite, chlorite, epidote ± plagioclase ± muscovite. Ore minerals < 2% (pyrite, hematite, sphalerite, chalcopyrite, and native gold).	Diameter ranges from several millimeters to 15 cm. Rarely occur in volcaniclastic rocks. Quartz-K-feldspar ratio variable. Vugs occur in all mines of the Nambija district. See also Figs. 3a, c and 4b, f.
Elongate vugs	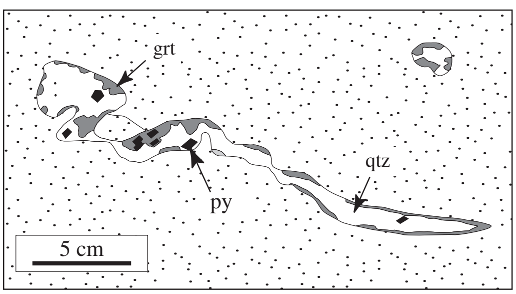		Width ranges from 1 mm to 15 cm, length up to a few meters (continuous transition to type I veins). They develop in places in volcaniclastic rocks but always within tens of centimeters of the skarn bodies. Best developed at Cambana, Campanillas, and Guaysimi. See also Fig. 3a.
Type I veins	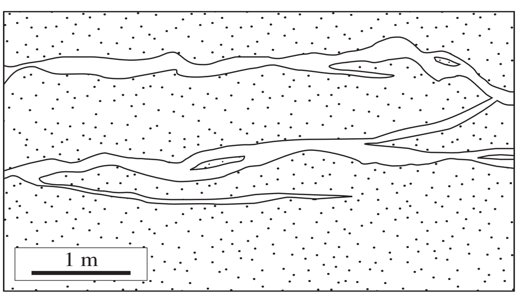		Widths range from 2 to 30 cm. Walls are better defined than in vugs particularly where cutting volcaniclastic rocks. Quartz-K-feldspar ratio is always >1:1. Highest gold grades. Typically well developed at Campanillas and to a lesser extent at Guaysimi and at Nambija, recognized at Cambana, but virtually absent at Fortuna. See also Figs. 3b, 4c, d, e, 7a, b.
Type II and Type III veins	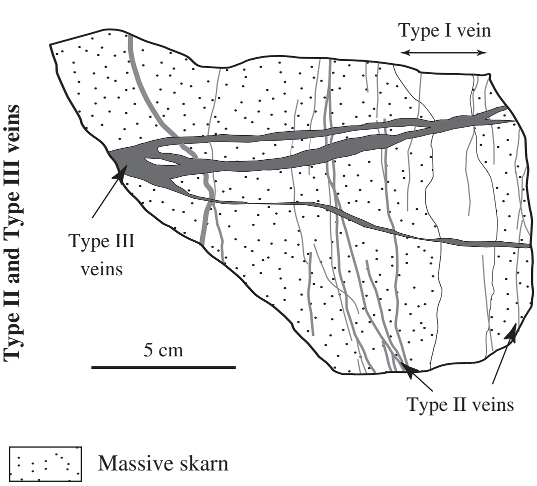	Throughgoing veins. **Filling:** similar mineralogy to type I veins but carbonates always present and sulfides more (II) to much more (III) abundant.	**Type II veins (N10-60°E)** They are thin (<1 mm) and occur mostly as bundles of parallel veins. Sulfide content <5%. Typically well developed in the Guaysimi Central mine. Occur sometimes at Campanillas and in El Tierrero mine. Always cut type I veins. See also Figs. 3b, c, 4f, and 7b. **Type III veins (N70-100°E)** Thickness is mainly in the range of 1 to 2 mm but up to a few cm. Sulfide content 5 to 50% (sphalerite and molybdenite observed). Well developped in the Katy area at Campanillas, in El Tierrero mine at Nambija, and at Guaysimi. Actinolite observed at Guaysimi Central.

FIG. 7. Main features of structurally controlled vugs and vein types in the Nambija district. Vugs and type I veins are interpreted as dilational features. Abbreviations: Au = gold, grt = garnet, kfs = K-feldspar, qtz = quartz, py = pyrite. See Figure 9b for typical internal structure of type I veins.

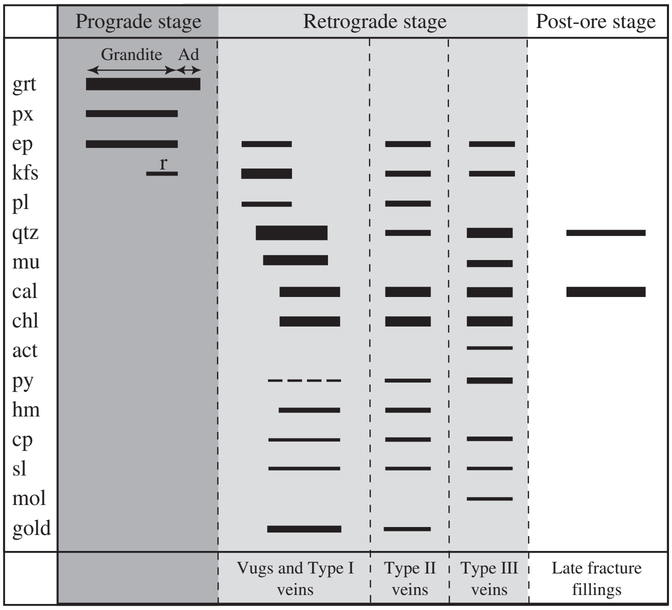

Ad: andraditic honey-yellow garnet
r: rims at contact skarn/volcaniclastic rock

FIG. 8. Schematic paragenetic chart of the Nambija district gold skarns. Abbreviations: act = actinolite, cal = calcite, chl = chlorite, cp = chalcopyrite, ep = epidote, grt = garnet, hm = hematite, kfs = K-feldspar, mol = molybdenite, mu = muscovite, pl = plagioclase, px = pyroxene, py = pyrite, qtz = quartz, sl = sphalerite.

salinities than those in late garnet (Fig. 11). As mentioned above, no suitable inclusions in the dominant but dirty brown garnet skarn were found. Similar temperatures, salinities, and V/L ratios (L1–L2) are observed in fluid inclusions in epidote as well as in those occurring as clusters in milky quartz (422°–345°C, 10.6–1.9 wt % NaCl equiv).

Homogenization temperatures of <300°C, mainly between 250° and 150°C, are observed in secondary L3 inclusions in milky quartz which display a wide salinity range (0.1–25 wt % NaCl equiv), with values clustered around 2 to 8 and 15 to 22 wt percent NaCl equiv. In the same temperature range, high-salinity Lh inclusions (31–44 wt % NaCl equiv) occur, in places, in clear pyramidal quartz of type I veins (Campanillas) and as secondary inclusions in milky quartz (Fortuna). The fluid inclusions in the calcite sealing in normal faults record low-temperature (94°–75°C) intermediate-salinity fluids (21.3–23.1 wt % NaCl equiv). Similar moderate to low temperatures and salinities were found in quartz and calcite by T. J. Shepherd (1988, *in* Litherland et al., 1994).

Re-Os Molybdenite Ages in Type III Veins

In the El Tierrero mine at Nambija, 2- to 5-cm-wide, skarn-hosted type III veins contain quartz, K-feldspar, epidote, calcite, pyrite, chalcopyrite, molybdenite, and/or sphalerite and cut vugs and type I veins. Two molybdenite samples from the type III veins were separated at AIRIE in Colorado and yielded Re-Os ages of 145.92 ± 0.46 and 145.58 ± 0.45

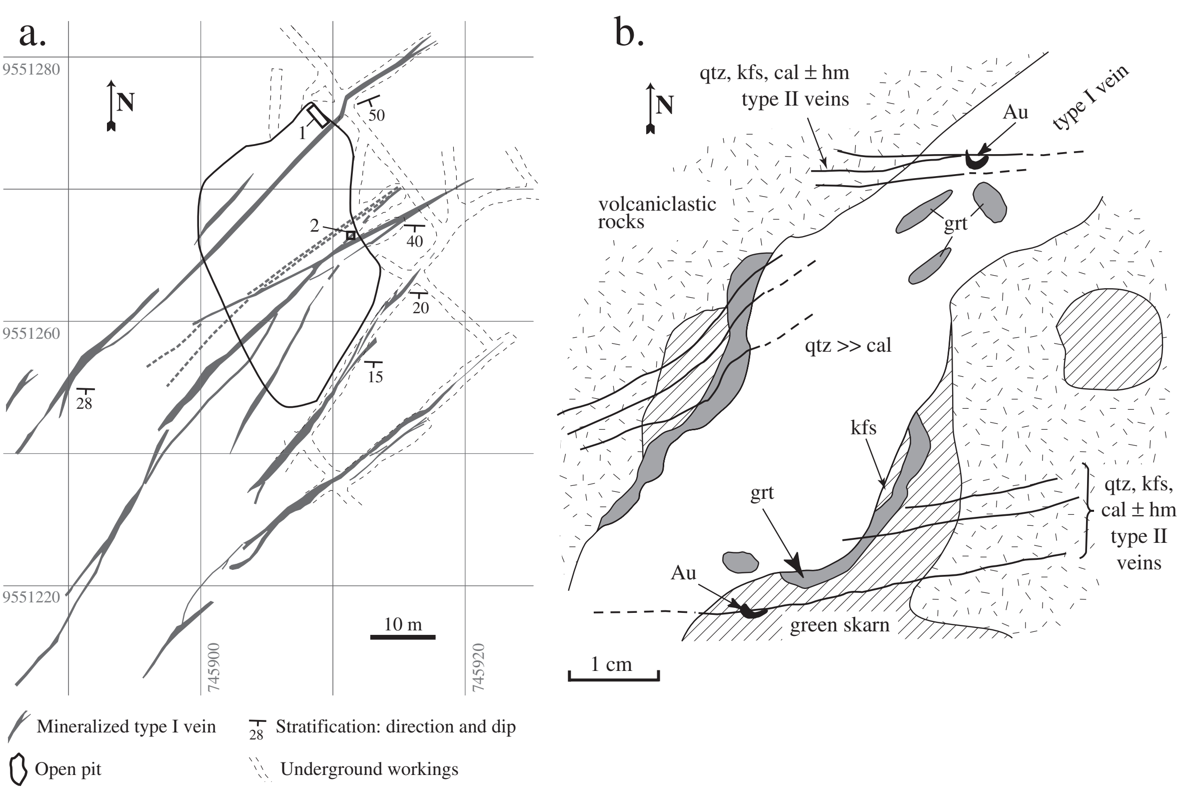

FIG. 9. a. Map of the Campanillas main open pit, showing steeply dipping mineralized type I veins. Inset 1 = location of detailed bench description shown in Figure 3b. Inset 2 = location of the sketch in (b). b. Sketch of a gold-bearing (Au) type I vein filled with garnet (grt), quartz (qtz), K-feldspar (kfs), and calcite (cal). The vein cuts volcaniclastic rocks and green skarn. Type II veins filled with calcite, quartz, K-feldspar, and hematite (hm) cut the rest.

Ma (H. Stein, AIRIE Colorado, *in* Vallance et al., in prep.). It should be pointed out that the dated molybdenite was not taken from molybdenite-bearing quartz-rich and sulfide-poor A or B veins crosscutting the El Tierrero porphyry (Prodeminca, 2000, p. 87) but in sulfide-rich type III veins crosscutting the skarn, which can be compared to D veins in a porphyry systems (see above).

Discussion and Conclusions

Skarn evolution

As in other skarns developed in volcaniclastic rocks (Newberry et al., 1997; L. Meinert, pers. commun., 2004), mineral zoning is not well defined in the Nambija district. The bedding-parallel form of most skarn bodies is explained by

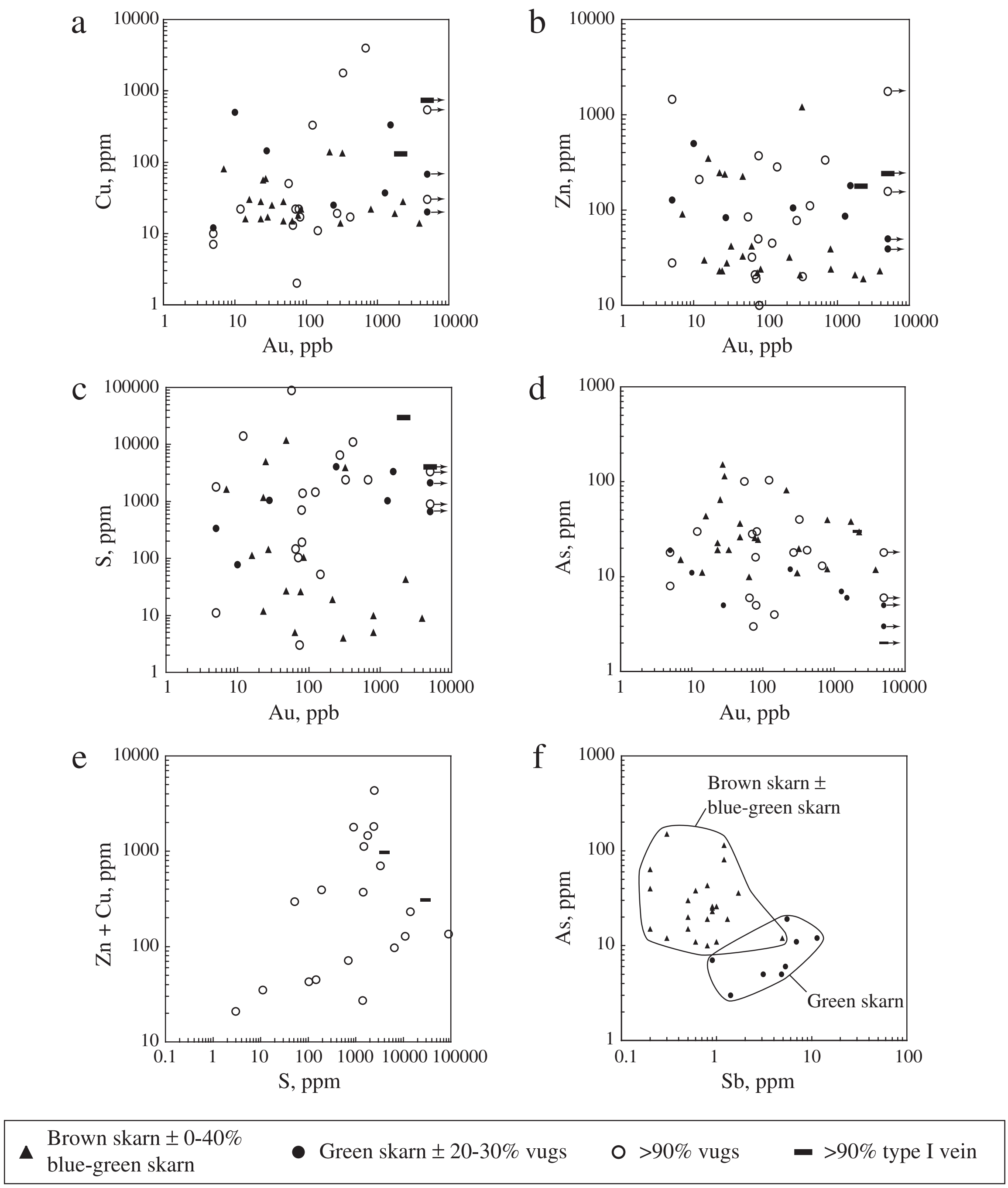

FIG. 10. Log-log plots of trace element analyses for selected mineralized samples from the Nambija district (see Table 2). No correlation is observable between (a) Au and Cu, (b) Au and Zn, (c) Au and S, and (d) Au and As. A positive correlation is observable between (e) S and Zn + Cu in vugs and type I veins. (f). Sb vs. As indicates a preferential spatial association of antimony with green skarn and arsenic with brown skarn ± blue-green skarn.

TABLE 2. Metal Contents in Selected Mineralized and Skarn Samples from the Nambija District

Sample no.	DTR361-1	DTR 190	DTR 207	DTR 179	DTR 397	DTR 380	DTR 105	DTR 367	DTR 411
Location	Guaysimi-Central	Campanillas	Fortuna		Cambana	Campanillas		Guaysimi-Central	
Description	Pure brown skarn	Brown skarn (60%) + blue-green skarn (40%)	Brown skarn (50%) + blue-green skarn (50%)	Green skarn (70%) + vugs (30%)	Green skarn (80%) + vugs (20%)	Vugs >90%		Type I vein >90%	
Au (ppm)	0.09	0.32	0.21	1.27	>5	>5	1,020	>5	2.12
Ag (ppm)	<5	<5	<5	<5	<5	6	25	20	<5
Cu (ppm)	22	135	140	37	68	54	375	730	130
Zn (ppm)	24	1,211	32	86	50	2,200	751	240	177
Pb (ppm)	13	61	23	15	14	25	8	11	46
As (ppm)	25	20	81	7	3	18	6	2	30
Sb (ppm)	0.9	0.5	1.2	0.9	1.4	0.8	1.7	2	0.7
Bi (ppm)	<0.5	1.7	0.6	1	9.4	<0.5	1.1	0.9	1.4
Te (ppm)	<0.5	0.7	0.5	0.6	1.3	<0.5	<0.5	<0.5	<0.5
S (%)	0.03	0.44	<0.01	0.14	0.06	0.09	0.18	0.4	2.95

Notes: Sample wt = 300 to 1,000 g; Au, Ag, As, and Sb analyzed by neutron activation (Xral, Toronto, Canada); Au in sample DTR 105 was analyzed by fire assay (Xral, Toronto, Canada); Cu and Pb analyzed by standard XRF (Lausanne University, Switzerland); Cu, Zn, Pb, and S analyzed by standard free semiquantitative analyses on powder, using Uniquant software (Lausanne University, Switzerland); Bi and Te analyzed by atomic absorption (Xral, Toronto, Canada)

differences in permeability and reactivity of the Triassic Piuntza unit. The dominance of garnet over pyroxene is characteristic of oxidized gold skarns (Meinert, 1998). The observed evolution from granditic to andraditic compositions with time, a common feature in many skarns, may be due to progressively more oxidizing conditions, lower temperatures of formation, and/or salinity decreases (Einaudi et al., 1981; Jamtveit et al, 1995; Newberry et al., 1997).

A salient feature of the Nambija skarn is the poor imprint of the retrograde stage, which does not affect most of the massive brown garnet skarn, is only slightly better expressed in the green pyroxene-epidote skarn, and is mainly developed as infill of structurally controlled (N10°–60°E) vugs and veins and in an intergranular position in the transitional blue-green garnet skarn. The mineral association of the retrograde skarn, milky quartz, K-feldspar, calcite, chlorite, hematite, and/or pyrite is typical for oxidized gold skarn deposits (e.g., Red Dome, Australia, and Mc Coy, Nevada; Ewers and Sun, 1989; Brooks et al., 1991; Meinert, 1998). The general absence of corrosion of garnet borders, including those on vug and type I vein walls, suggests a continuous process encompassing both the prograde and retrograde stages.

Fluid

Given the impossibility of obtaining fluid inclusion data from the brown skarn garnet, the high-temperature (up to 580°C), high-salinity (up to 60 wt % NaC equiv) fluid inclusions in pyroxene represent the best approximation to the fluid conditions during a significant part of the main prograde stage. Such a highly saline fluid could have been segregated directly from a magma at 200 MPa (Cline and Bodnar, 1991) or, alternatively, it may be interpreted as the result of boiling of a moderately saline (~8–10 wt % NaCl equiv) magmatic fluid (Burnham, 1979) at temperatures of ~500°C. We prefer the second explanation because there is no trace of high-salinity fluid in the paragenetically later garnet. The moderately saline fluid may correspond to contraction of a vapor separated at depth from magmatic fluid, as proposed by Heinrich (2003) for some porphyry copper systems or, alternatively, to the magmatic fluid itself, which would not have undergone boiling because it did not intersect the solvus along the cooling path, as suggested by Meinert et al. (1997) for the Big Gossan skarn deposit.

The moderate- to low-salinity L1 and L2 fluid inclusions (20–2 wt % NaCl equiv) in paragenetically later garnet as well as in epidote and quartz from vugs and type I veins may represent trapping, at a later stage and slightly lower temperature (420°–350°C), of similar moderately saline fluids with or without some degree of boiling and mixing. The similarity in salinities and homogenization temperatures between L1 and L2 fluid inclusions in late garnet, epidote, and quartz is consistent with the apparent continuum between the prograde and retrograde stages suggested by petrographic observations.

The wide salinity range in secondary liquid-rich L3 and Lh fluid inclusions in quartz, with homogenization temperatures of ~200°C, may point to mixing of saline to moderately saline fluid with meteoric water, perhaps combined with posttrapping modification leading to salinity increase (Audetat and Günther, 1999). A boiling hypothesis is unlikely, as it would require unrealistically low pressures. We do not have good

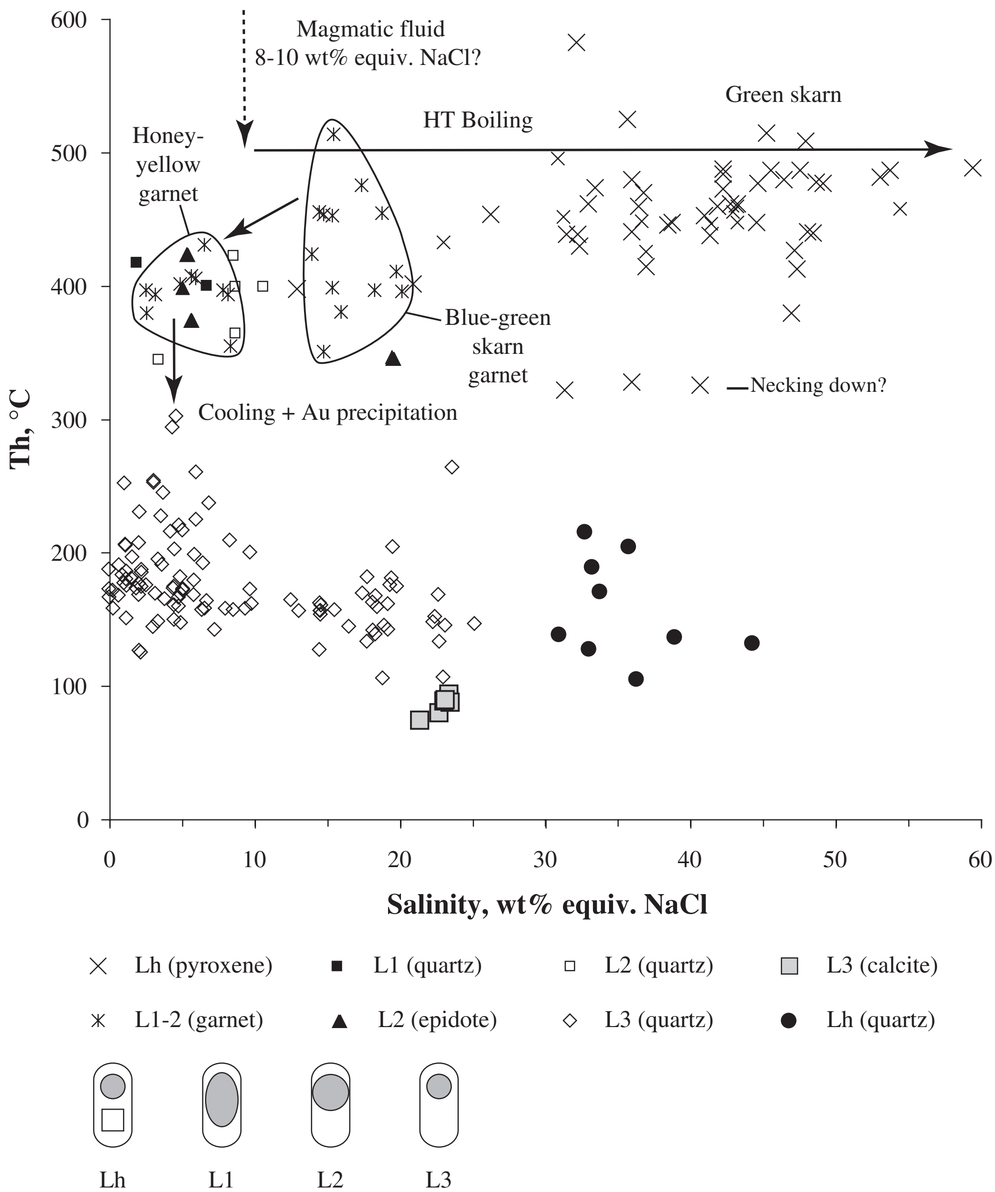

FIG. 11. T_h vs. salinity diagram for samples from the Fortuna (n = 63), Cambana (n = 34), Campanillas (n = 44), Nambija (n = 19), and Guaysimi (n = 62) mines and sketch of the different fluid inclusion types. Epidote and quartz are from vug and type I vein fillings, calcite from the late normal faults, and other hosts as indicated. According to the criteria of Roedder (1984), fluid inclusions in pyroxene, garnet, and epidote are considered to be primary, L1 and L2 in quartz and L3 in calcite are probably primary, and L3 and Lh in quartz are secondary.

time constraints for these secondary quartz fluid inclusions: they may have formed much later and by different processes than the skarn mineralization. The presence in the late calcite sealing normal faults of low-temperature (94°–75°C) fluid inclusions with salinities of ~21 to 23 wt percent NaCl equiv suggests ingress of sedimentary brine. Such brine could also have contributed to the secondary fluid inclusions in quartz.

Paragenetic position of gold and its precipitation

Gold is spatially associated with the retrograde alteration. This is observed at both orebody and outcrop scales, as only areas affected by retrograde alteration are mineralized, as well as both at sample and microscopic scales, with gold infillings of vugs and N10°E- to N60°E-trending types I and II veins in the same paragenetic position as retrograde milky quartz, K-feldspar, chlorite, and calcite.

These observations imply gold precipitation during the retrograde stage but not during the latest retrograde alteration, as indicated by an absence of gold in the sulfide-rich type III veins. At temperatures of 300° ± 50°C, gold can be transported as hydrosulfide or chloride complexes (Benning and Seward, 1996; Gammons and William-Jones, 1997; Gibert et al., 1998). The frequent association of gold-mineralized samples with high hematite/pyrite ratios and the general low sulfide and metal contents suggest high oxygen fugacity during gold deposition. The low sulfur and metal contents of mineralized samples from the Nambija skarns (S, Cu, Zn, and As contents typically <100 ppm; Sb, Bi, and Te <10 ppm) are comparable to those reported for the McCoy oxidized gold skarn (Meinert et al., 1990) but, for most elements, lower by a factor of 10 or more than those in the reduced gold skarns of Buckhorn Mountain, Washington (Hickey, 1992), Fortitude, Nevada (Meinert et al., 1990), Ortosa, Spain (Fuertes-Fuente et al., 2000), and some Alaskan deposits (Newberry et al., 1997). The oxidizing character of the fluid would favor gold transport as chloride complexes and precipitation by cooling. In contrast, the bonanza grades encountered at several places at Nambija and the lack of correlation between gold and base metals are difficult to explain simply in terms of cooling and point rather to rapid destabilization of gold-bearing complexes. However, there are no indications of precipitation by destabilization of hydrosulfide complexes, as gold deposition is not accompanied by oxidation nor by a distinct sulfide phase that could have destabilized the complex.

Age and relationship to magmatic activity and tectonics

The Re-Os ages (145.92 ± 0.46 and 145.58 ± 0.45 Ma) obtained on molybdenite from sulfide-rich type III veins at Nambija-El Tierrero are minimum ages for the gold mineralization, as the sampled type III veins cut vugs and type I veins and elsewhere in the district, type III veins also cut type II veins. These ages coincide within error with the 141 ± 5 Ma K-Ar hornblende age reported by Prodeminca (2000) for the quartz monzonite porhyry intrusion at the Cumay Cu-Mo prospect (Fig. 2) and are slightly younger than K-Ar ages of 154 ± 5 Ma (whole rock) and 157 ± 5 Ma (hornblende) obtained at San Carlos and Panantza, 70 km to the north of the Nambija district, from felsic porphyry intrusions from the Late Jurassic Pangui porphyry copper belt (Fig. 1; Gendall et al., 2000; Prodeminca, 2000). Like the Nambija district, the porphyry intrusions of the Pangui belt crosscut the Zamora batholith. Much younger K-Ar ages on vein (Cumay) and alteration minerals (El Tierrero) obtained by Prodeminca (2000) may be the result of disturbance.

The similar mineralogic compositions and evolution of geometric characteristics may suggest that type III veins were formed during the last stages of the retrograde event as part of the same cooling process during which veins developed increasingly sharp boundaries, sulfide contents augmented, and wall-rock alteration became more important. If this assumption is correct, the molybdenite Re-Os ages of ~146 Ma would be not only minimum ages but also closely date the gold mineralization, which, according to the imprecise K-Ar age, would be coeval with the Cumay porphyry intrusion. Therefore it is tentatively proposed that the Nambija gold skarn is related to Late Jurassic porphyry intrusions that cut the Mid-Jurassic Zamora batholith. However, it is also possible that a time gap exists between types I and II and type III veins, which could also explain their different orientations (N10°–60°E and N70°–100°E, respectively). Additional age determinations and mapping of crosscutting relationships between skarns, felsic porphyry intrusions, and alteration attributed to them are necessary to clarify this point and also determine if the porphyry intrusions belong to late phases of the Zamora batholith or constitute an independent magmatic event.

Lead isotope compositions of sulfide minerals from the Nambija skarns (Chiaradia et al., 2004) partly overlap those of the Jurassic Zamora batholiths and porphyries from the Nambija district, supporting derivation of at least part of the lead in the Nambija mineralization from Jurassic magmas.

The results reported herein do not support the genetic interpretation of Prodeminca (2000) for the origin of the Nambija gold deposits. According to Prodeminca (2000, p. 182), the Piuntza unit was metamorphosed by contact with the Zamora batholith during the Jurassic, with local development of clinopyroxene skarn. Extensive grandite skarn would only have developed concomitantly with emplacement of mid-Cretaceous porphyry copper stocks. Based mainly on K-Ar dates for K-feldspar, it is further claimed that gold precipitated under epithermal conditions (p. 89) during the Late Cretaceous and/or Paleocene in northeast-trending faults and veins, in part as the result of remobilization of skarn components.

Our results confirm the northeasterly structural control, the main direction of the gold-bearing vugs, and types I and II veins. However, this structural direction was not a late addition but already existed at the end of the prograde stage, as a control of the dilational fillings represented by the vugs and type I veins, and was perpetuated during the retrograde stage as shown by the development of the throughgoing type II veins. In other words, skarn development, including gold deposition during the retrograde stage, took place during conditions of tectonic stress. The N10° to 60°E orientations of vugs and type I and II veins are also compatible with the regional northeasterly structures (Fig. 2), in part described as tensional fractures (Prodeminca, 2000), and with a stress field controlled by northeast-directed subduction as prevailed during the Late Jurassic (Litherland et al., 1994). This scenario accords with the minimum Re-Os age of ~146 Ma for skarn and gold mineralization.

Acknowledgments

We thank Comcumay S.A., Cominza S.A, Compañía Minera del Ecuador-Andos, Compañía Minera Sol de Oriente, Cooperativa Once de Julio, and Fortuna Gold Mining Corporation for access to their mines and properties and for assistance in the field. This paper benefited from discussions with L. Meinert, F. Tornos, and C. Heinrich and thorough reviews by R. Newberry, Peter Pitfield, and Richard Sillitoe. The investigation was supported by the Swiss National Science Foundation, as project 2000-062 000.00.

REFERENCES

Aguirre, L., 1992, Metamorphic pattern of the Cretaceous Celica Formation, SW Ecuador, and its geodynamic implications: Tectonophysics, v. 205, p. 223–237.

Aguirre, L., and Atherton, M.P., 1987, Low-grade metamorphism and geotectonic setting of the Macuchi Formation, Western Cordillera of Ecuador: Journal of Metamorphic Geology, v. 5, p. 473–494.

Aspden, J.A., and Litherland, M., 1992, The geology and Mesozoic collisional history of the Cordillera Real, Ecuador: Tectonophysics, v. 205, p. 187–204.

Audetat, A., and Günther, D., 1999, Mobility and H_2O loss from fluid inclusions in natural quartz crystals: Contributions to Mineralogy and Petrology, v. 137, p. 1–14.

Benning, L.G., and Seward, T.M., 1996, Hydrosulphide complexing of gold (I) in hydrothermal solutions from 150 to 400°C and 1500 bars: Geochimica et Cosmochimica Acta, v. 60, p. 1849–1871.

Brooks, J.W., Meinert, L.D., Kuyper, B.A., and Lane, M.L., 1990, Petrology and geochemistry of the McCoy gold skarn, Lander County, NV: Geology and Ore Deposits of the Great Basin, Geological Society of Nevada Symposium, Reno, 1990, Proceedings, v. 1, p. 419–442.

Burnham, C.W., 1979, Magmas and hydrothermal fluids, *in* Barnes, H.L., ed., Geochemistry of hydrothermal ore deposits, 2nd ed.: New York, John Wiley, p. 71–136.

Chiaradia, M., Fontboté, L., and Paladines, A., 2004, Metal sources in mineral deposits and crustal rocks of Ecuador (1°N–4°S): A lead isotope synthesis: Economic Geology, v. 99, in press.

Cline, J.S., and Bodnar, R.J., 1991, Can economic porphyry copper mineralization be generated by a typical calc-alkaline melt?: Journal of Geophysical Research, v. 96, p. 8113–8126.

Cooperativa 11 julio and Gribipe, 2000, Concession Minera Nambija 1, Informe final de exploración, 20 p.

Einaudi, M.T., Meinert, L.D., and Newberry, R.J., 1981, Skarn deposits: Economic Geology 75th Anniversary Volume, p. 317–391.

Ewers, G.R., and Sun, S.S., 1989, Genesis of the Red Dome gold skarn deposit, northeast Queensland: Economic Geology Monograph 6, p. 218–232.

Feininger, T., 1987, Allochthonous terranes in the Andes of Ecuador and northwestern Peru: Canadian Journal of Earth Sciences, v. 24, p. 266–278.

Fuertes-Fuente, M., Martin-Izard, A., Nieto, J.G., Maldonado, C., and Varela, A., 2000, Preliminary mineralogical and petrological study of the Ortosa Au-Bi-Te ore deposit: A reduced gold skarn in the northern part of the Rio Narcea gold belt, Asturias, Spain: Journal of Geochemical Exploration, v. 71, p. 177–190.

Gammons, C.H., and Williams-Jones, A.E., 1997, Chemical mobility of gold in the porphyry-epithermal environment: Economic Geology, v. 92, p. 45–59.

Gendall, I.R., Quevedo, L.A., Sillitoe, R.H., Spencer, R.M., Puente, C.O., Leon, J.P., and Povedo, R.R., 2000, Discovery of a Jurassic porphyry copper belt, Pangui area, southern Ecuador: Society of Economic Geologists Newsletter 43, p. 1, 8–15.

Gibert, F., Pascal, M.L., and Pichavant, M., 1998, Gold solubility and speciation in hydrothermal solutions: Experimental study of the stability of hydrosulphide complex of gold (AuHS°) at 350 to 450°C and 500 bars: Geochimica et Cosmochimica Acta, v. 62, p. 2931–2947.

Gustafson, L.B., and Hunt, J.P., 1975, The porphyry copper deposit at El Salvador, Chile: Economic Geology, v. 70, p. 856–912.

Hammarstrom, J.M., 1992, Mineralogy and chemistry of gold-associated skarn from Nambija, Zamora province, Ecuador: A reconnaissance study: Advances related to U.S. and international mineral resources: U.S. Geological Survey Bulletin, v. 2039, p. 107–118.

Heinrich, C.A., 2003, Magmatic vapour condensation and the relation between porphyries and epithermal Au-(Cu-As) mineralisation: Thermodynamic constraints: Mineral Exploration and Sustainable Development, Society for Geology Applied to Mineral Deposits Biennal Meeting, 7th, Athens, 2003, Proceedings, p. 279–282.

Hickey, R.J., 1992, The Buckhorn Mountain (Crown Jewel) gold skarn deposit, Okanogan County, Washington: Economic Geology, v. 87, p. 125–141.

Jamtveit, B., Ragnarsdottir, K.V., and Wood, B.J., 1995, On the origin of zoned grossular-andradite garnets in hydrothermal systems: European Journal of Mineralogy, v. 7, p. 1399–1410.

Litherland, M., Aspden, J.A., and Jemielita, R.A., 1994, The metamorphic belts of Ecuador: British Geological Survey Overseas Memoir 11, 147 p.

Markowski, A., 2003, The gold skarn of Fortuna, (Nambija district, Cordillera del Cóndor, Ecuador): Unpublished M.Sc. thesis, Geneva, University of Geneva, 184 p. (http://www.unige.ch/sciences/terre/mineral/).

Meinert, L.D., 1998, A review of skarns that contain gold: Mineralogical Association of Canada Short Course Series, v. 26, p. 359–414.

Meinert, L.D., Brooks, J.W., and Myers, G. L., 1990, Whole rock geochemistry and contrast among skarn types: Great Basin Symposium, Geology and Ore Deposits of the Great Basin, Geological Society of Nevada Fieldtrip 2 Guidebook, p. 179–192.

Meinert, L.D., Hefton, K.K., Mayes, D., and Tasiran, I., 1997, Geology, zonation, and fluid evolution of the Big Gossan Cu-Au skarn deposit, Ertsberg district, Irian Jaya: Economic Geology, v. 92, p. 509–533.

Mining Magazine, 1990, Campanilla gold mine, v. 163, p. 322–323.

Mourier, T., Laj, C., Mégard, F., Roperch, P., Mitouard, P., and Farfan Medrano, A., 1988a, An accreted continental terrane in northwestern Peru: Earth and Planetary Science Letters, v. 88, p. 182–192.

Mourier, T., Mégard, F., Reyes Rivera, L., and Pardo Arguedas, A., 1988b, L'évolution mésozoïque des Andes de Huancabamba (nord Pérou-sud Equateur) et l'hypothèse de l'accrétion du bloc Amotape-Tahuin: Bulletin de la Société Géologique de France, v. 3, p. 69–79.

Newberry, R.J., Allegro, G. L., Cutler, S.E., Hagen-Leveille, J.H., Adams, D.D., Nicholson, L.C., Weglarz, T.B., Bakke, A.A., Clautice, K.H., Coulter, G.A., Ford, M.J., Myers, G.L., and Szumigala, D.J., 1997, Skarn deposits of Alaska: Economic Geology Monograph 9, p. 355–395.

Paladines, A., and Rosero, G., 1996, Zonificación mineralogénica del Ecuador: Quito, edición Laser, 146 p.

Prodeminca, 2000, Depositos porfidicos y epi-mesotermales relacionados con intrusiones de la Cordillera del Cóndor: Evaluacion de distritos mineros del Ecuador: Unidad de Coordinación del Proyecto Prodeminca Proyecto MEM BIRF 36-55 EC, v. 5, 223 p.

Roedder, E., 1984, Fluid inclusions: Reviews in Mineralogy, v. 12, 644 p.

Salazar, E., 1988, Nambija-Conocimiento geologico y mineralogico hasta al presente: Quito, Instituto Ecuatoriano de Minería, unpublished report, 11 p.

Shepherd, T.J., 1981, Temperature programmable heating-frezing stage for microthermometric analysis of fluid inclusions: Economic Geology, v. 76, p. 1244–1247.

Vallance, J., Markowski, A., Fontboté, L., and Chiaradia, M., 2003, Mineralogical and fluid inclusion constraints on the genesis of gold-skarn deposits in the Nambija district (Ecuador): Mineral Exploration and Sustainable Development, Society for Geology Applied to Mineral Deposits Biennal Meeting, 7th, Athens, 2003, Proceedings, p. 399–402.

van Thournout, F., Hertogen, J., and Quevado, L., 1992, Allochthonous terranes in northwestern Ecuador: Tectonophysics, v. 205, p. 205–221.